ABUAD Journal of Engineering Research and Development (AJERD) ISSN: 2645-2685
Volume 1, Issue 2, 205-210

Optimised Gain Saturated Pre-Amplified Free-Space Optical Communication Systems

Jeremiah Oluwatosin BANDELE[1,*], Samson Olasunkanmi ADIGUN[1]

[1]*Department of Electrical/Electronics and Computer Engineering, College of Engineering, Afe Babalola University, Ado-Ekiti, Ekiti State, Nigeria*
jbandele@abuad.edu.ng/adigunso@abuad.edu.ng

[*]*Corresponding Author: jbandele@abuad.edu.ng*

Date of First Submission: 27/04/2018
Date Accepted: 01/06/2018

Abstract*: The performance of a fixed and saturated gain preamplified free-space optical communication system in a turbulent atmosphere is investigated, in the presence of amplified spontaneous emission noise. Bit error rate (BER) analysis of both non-adaptive decision and adaptive decision threshold schemes are considered and the effects of using both fixed and saturated gain preamplified receivers are investigated for different turbulence regimes. Results obtained in this paper showed, as expected, that the lognormal distribution gives a better performance than the gamma-gamma distribution in the weak turbulence regime and that the BER performances reaches an optimal level when the power at the preamplifier input is comparable with the internal saturation power of the preamplifier. Also, it is shown that the optimal non-adaptive decision threshold in a gain saturated preamplified receiver will have a decision threshold level between 0.2 and 0.3.*

Keywords: *Free-space optical communication, atmospheric turbulence, optical amplifier, gain saturation, decision threshold.*

1. INTRODUCTION

Free-space optical (FSO) communication has attracted significant interest in research and development activities because of the advantages it offers compared to radio frequency (RF) and optical fibre communication systems [1-7]. Despite all the possible benefits of deploying FSO systems, their capabilities are limited by atmospheric conditions [8-10]. A major impairment to seamless signal transmission through the atmosphere is thermal inhomogeneity. These thermal inhomogenities cause random temporal and spatial refractive index changes which results in large-scale and small-scale eddies (i.e. atmospheric turbulence) that haphazardly interacts with the transmitted optical signal [8, 11]. Atmospheric turbulence causes scintillation (i.e. fluctuations of the optical signal transmitted through the atmosphere) and it significantly affects system performance [11]. These undesirable effects are even more pronounced when an FSO system is required for longer distances [12]. Specifically, the effect of atmospheric turbulence is highly significant at communication distances greater than 1 km [6, 13]. In order to obtain the desired performance especially over long distances, suitable turbulence alleviation methods are required such as using error correcting codes with interleaving [14], aperture averaging [15] and spatial diversity [6].

As shown in an earlier work [16], the ability of an optical amplifier (OA) to adapt its gain to new power levels by providing lower gain to higher input powers and higher gains to lower input powers makes it suitable for scintillation mitigation in a FSO communication system. These saturation characteristics of the OA gain was also shown to enhance acceptable bit error rate (BER) performances where channel state information is not known and a non-adaptive decision threshold is used at the receiver [16].

Using the Gaussian Approximation (GA) technique, the performance evaluation of fixed and saturated gain preamplified receivers in a non-return-to-zero (NRZ) on-off keying (OOK) FSO communication system is considered in this work. Results are shown for various threshold settings and various statistical models are used to model the different atmospheric turbulence levels. Also, the optimum non-adaptive decision threshold when a saturated gain preamplifier is deployed at the receiver is presented. Note that only single wavelength FSO communication systems are considered in this paper. After this introductory part, the turbulence models used to represent the FSO link is described in section 2. Section 3 describes an optically preamplified FSO receiver model. In Section 4, effects of gain saturation in the preamplifier and the bit error rate (BER) analysis are presented. Results of the numerical analysis are discussed in section 5 and a conclusion is given in section 6.

2. CHANNEL STATISTICS

Various statistical channel models have been used to describe atmospheric-induced turbulence fading. The lognormal (LN) distribution is commonly used to characterise the weak turbulence regime and the K

distribution (which is consistent with experimental results) is used to characterise the strong turbulence regime. Compared to the LN distribution, the gamma-gamma (GG) distribution used to characterise the weak to strong turbulence regimes shows better agreement between experimental and theoretical data. In a saturated turbulence regime, the negative exponential (NE) distribution has proved to give a better fit when compared with theoretical data. The probability density functions (PDFs) of the various atmospheric turbulence distributions are given in Table 1 [17, 18].

Table 1: Atmospheric turbulence distributions

Model	PDF	Definitions
Gamma-gamma	$f_{GG_{h_t}}(h_t)=\frac{2(\alpha\beta)^{(\alpha+\beta)/2}}{\Gamma(\alpha)\Gamma(\beta)}h_t^{\left(\frac{\alpha+\beta}{2}\right)-1}K_{\alpha-\beta}\left(2\sqrt{\alpha\beta h_t}\right)$	$\alpha=\left\{\exp\left[\frac{0.49\sigma_R^2}{\left(1+\left(1.11\sigma_R^{12/5}\right)\right)^{7/6}}\right]-1\right\}^{-1}$
Lognormal	$f_{LN_{h_t}}(h_t)=\frac{1}{h_t\sqrt{2\pi\sigma_l^2}}\exp\left\{-\frac{\left[\ln(h_t)+\frac{1}{2}\sigma_l^2\right]^2}{2\sigma_l^2}\right\}$	$\beta=\left\{\exp\left[\frac{0.51\sigma_R^2}{\left(1+\left(0.69\sigma_R^{12/5}\right)\right)^{5/6}}\right]-1\right\}^{-1}$
K	$f_{K_{h_t}}(h_t)=\frac{2\alpha}{\Gamma(\alpha)}(\alpha h_t)^{\left(\frac{\alpha-1}{2}\right)}K_{\alpha-1}\left(2\sqrt{\alpha h_t}\right)$	$\sigma_l^2=\exp\left[\frac{0.49\sigma_R^2}{\left(1+\left(1.11\sigma_R^{12/5}\right)\right)^{7/6}}+\frac{0.51\sigma_R^2}{\left(1+\left(0.69\sigma_R^{12/5}\right)\right)^{5/6}}\right]-1$
Negative exponential	$f_{NE_{h_t}}(h_t)=\exp(-h_t)$	$\sigma_R^2=1.23C_n^2k^{7/6}D^{11/6}$

In Table 1, the paramater h_t is used to describe the varying channel loss (or gain) due to atmospheric turbulence. α and β are the number of large and small scale eddies due to the scattering process respectively, $\Gamma(.)$ is the Gamma function and $K_u(.)$ is the modified Bessel function of the second kind with order, u. σ_R^2, the Rytov variance is used to describe the different turbulence regimes. D is the length of the FSO link and $k=2\pi/\lambda$ represents the optical wave number where λ is the optical wavelength. C_n^2 is the refractive index structure parameter [17, 18].

3. OPTICALLY PREAMPLIFIED FSO RECEIVER MODEL

A FSO link with an optically preamplified FSO receiver model using a direct detection scheme with NRZ-OOK modulation is shown in Figure 1. The amplified spontaneous emission (ASE) noise produced is reduced with an optical band pass filter (OBPF). A photodiode (PD) of responsivity $R=\eta q/h\nu$ where h is the Planck constant, η is the quantum efficiency, q is the electronic charge and ν is the frequency of the optical carrier is used for optical-to-electrical (O/E) conversion of the transmitted signal before electrical amplification, filtering and the recovery of the transmitted data bit at the decision circuit [18, 19].

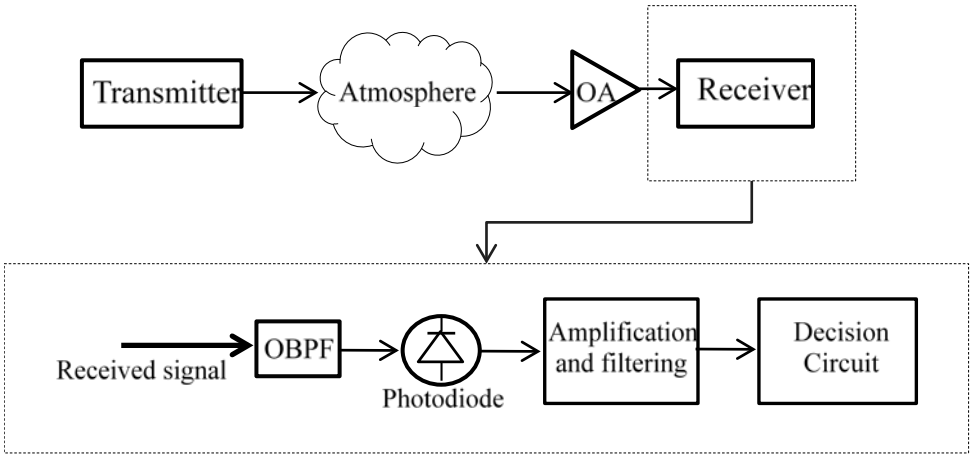

Figure 1: Single wavelength FSO link with an optically preamplified FSO receiver model

4. GAIN SATURATION AND BER ANALYSIS

The instantaneous signal power at the input of the OA is unconditionally related to its gain and the relation is given as [20]

$$P_{in} = \frac{P_{sat}}{G-1}\ln\left(\frac{G_{ss}}{G}\right) \quad (1)$$

where $P_{in} = P_{OAin_{av}} h_t$. $P_{OAin_{av}}$ is the turblence-free average power at the OA input. G_{ss} is the fixed (small signal) gain of the OA, P_{sat} is the internal saturation power of the OA and G is the operating (non-fixed) gain of the OA. In a FSO link where it is assumed that atmospheric fluctuations are appropriately tracked by the gain dynamics, this relationship between the gain and instantaneous input signal power of the OA describes a gain adjustment process where lower input powers receive higher gains and higher input powers receive lower gains leading to a more stable average power at the output of the OA given as [16]

$$P_{out}(P_{in}) = G(P_{in})P_{in} \quad (2)$$

Therefore, when a gain saturated OA is placed after the FSO link, a non-adaptive decision threshold can be easily used at the receiver since a more stable power is obtained at the OA output. The non-adaptive decision threshold, assumed set to a long term average received power at the photodiode, is obtained by averaging the OA output power over the turbulence PDF and it is given as [16]

$$i_D(P_{OAin_{av}}) = R\int_0^{\infty} P_{out}(P_{OAin_{av}} h_t) f_{atm}(h_t)\,dh_t \quad (3)$$

where *atm* refers to the statistical channel model. The adaptive decision threshold is given as [16].

$$i_D = \frac{\sigma_1 i_0(P_{OAin_{av}}, h_t) + \sigma_0 i_1(P_{OAin_{av}}, h_t)}{\sigma_1 + \sigma_0} \quad (4)$$

where the mean signal level at the sampling instant $i_x = GRP_{OAin_x}$ for transmitted data bits, $x \in \{0,1\}$ and P_{OAin_x} is the OA input power. The power in a 1 bit $P_{OAin_1} = \frac{2r}{r+1}P_{OAin_{av}}$, the extinction ratio $r = P_{OAin_1}/P_{OAin_0}$ and the power in a 0 bit $P_{OAin_0} = \frac{2}{r+1}P_{OAin_{av}}$. The total noise current variance $\sigma_x^2 = \sigma_{sx-sp}^2 + \sigma_{sp-sp}^2 + \sigma_{sh,x}^2 + \sigma_{th}^2$ where σ_{th}^2 is the receiver thermal noise variance, $\sigma_{sh,x}^2 = 2qR(GP_{OAin_x} + m_t N_0 B_{opt})B_e$ is the shot noise, $\sigma_{sx-sp}^2 = 4GR^2 P_{OAin_x} N_0 B_e$ is the signal-spontaneous beat noise, $\sigma_{sp-sp}^2 = 2m_t R^2 N_0^2 B_{opt} B_e\left(1 - \frac{B_e}{2B_{opt}}\right)$ is the spontaneous-spontaneous beat noise, B_{opt} is the OBPF bandwidth, $B_e = 0.7R_b$ is the receiver noise equivalent bandwidth, R_b is the bit rate, m_t is the number of polarisation states parameter (1 or 2), $N_0 = \frac{1}{2}(NFG-1)h\nu$ is the power spectral density of the ASE noise and NF is the noise figure.

The BER (obtained by making a Gaussian approximation assumption for the noise), conditioned on h_t, is given as [21]

$$BER(P_{OAin_{av}}) = \frac{1}{2}\left[\frac{1}{2}\mathrm{erfc}\left(\frac{i_D - i_0(P_{OAin_{av}})}{\sqrt{2\sigma_0^2(P_{OAin_{av}})}}\right) + \frac{1}{2}\mathrm{erfc}\left(\frac{i_1(P_{OAin_{av}}) - i_D}{\sqrt{2\sigma_1^2(P_{OAin_{av}})}}\right)\right] \quad (5)$$

The average BER obtained by averaging the conditioned BER over the turbulence PDF is given as [18]

$$BER_{av}(P_{OAin_{av}}) = \int_0^{\infty} BER(P_{OAin_{av}}) f_{atm}(h_t)\,dh_t \quad (6)$$

The non-adaptive decision threshold shown in (3) is equivalent to when the decision threshold level, D_{rel} is fixed midway between i_1 and i_0. This decision threshold can be regarded as corresponding to D_{rel} = 0.5. The optimum non-adaptive decision threshold can then be obtained as

$$i_{D_{opt}} = \Lambda(BER_{av,D_{rel}}(P_{OAin_{av}})) \quad D_{rel} = 0,..,1 \quad (7)$$

where $\Lambda(.)$ is an abbreviation for the mathematical minimum.

5. RESULTS AND DISCUSSIONS

Table 2 shows the parameters used for the numerical analysis. The saturated operation uses complete saturation characteristics and integrates the effect of ASE noise. An OA that cannot be driven into gain saturation ($P_{sat} \to \infty$) is referred to as a fixed gain OA and an OA that can be driven into gain saturation (P_{sat} = 5 dBm) is referred to as a saturated gain OA.

Table 2: General parameters used for numerical analysis

Parameter	Symbol	Value
optical wavelength	λ	1550 nm
bit rate	R_b	2.5 Gb/s
OBPF bandwidth	B_{opt}	70 GHz
noise figure	NF	5 dB
quantum efficiency	η	0.8
extinction ratio	r	10 dB

The receiver thermal noise (i.e. 7×10^{-7} A) is obtained with a baseline receiver sensitivity of -23 dBm corresponding to a BER of 10^{-12} [18]. The values used to

model the weak to strong turbulence regimes in Figure 2 are shown in Table 3.

Table 3: Parameters used to model the turbulence regimes

Parameter	Atmospheric turbulence regimes			
	Weak	Moderate	Strong	Saturated
σ_R^2	0.1	1.5	3.5	30
α	21.59	4.05	4.23	8.65
β	19.82	1.98	1.36	1.02

Figure 2 shows the BER curves for different turbulence regimes in a single wavelength FSO link. In Figure 2(a) where a fixed gain preamplified receiver with an adaptive decision threshold is used, the LN distribution is used to describe the weak turbulence regime and the GG distribution is used to describe the weak, moderate, strong and saturated turbulence regimes. As mentioned in [8, 18, 22] and shown in Figure 2(a), the LN distribution (BER of 10^{-12} achievable with a received optical power of about 36dBm) gives a better performance when compared to the GG distribution (BER of 10^{-12} achievable with a received optical power of about 34dBm) in the weak turbulence regime. However, the GG distribution has been shown to be more accurate when both are compared with experimental results [8, 18, 22, 23]. Also, as the turbulence strength decreases from the saturated turbulence regime to the weak turbulence regime, the BER performance becomes better. This increase in BER performance occurs because when the turbulence strength reduces, there is a proportional decrease in the fluctuation of the received optical signal at the receiver.

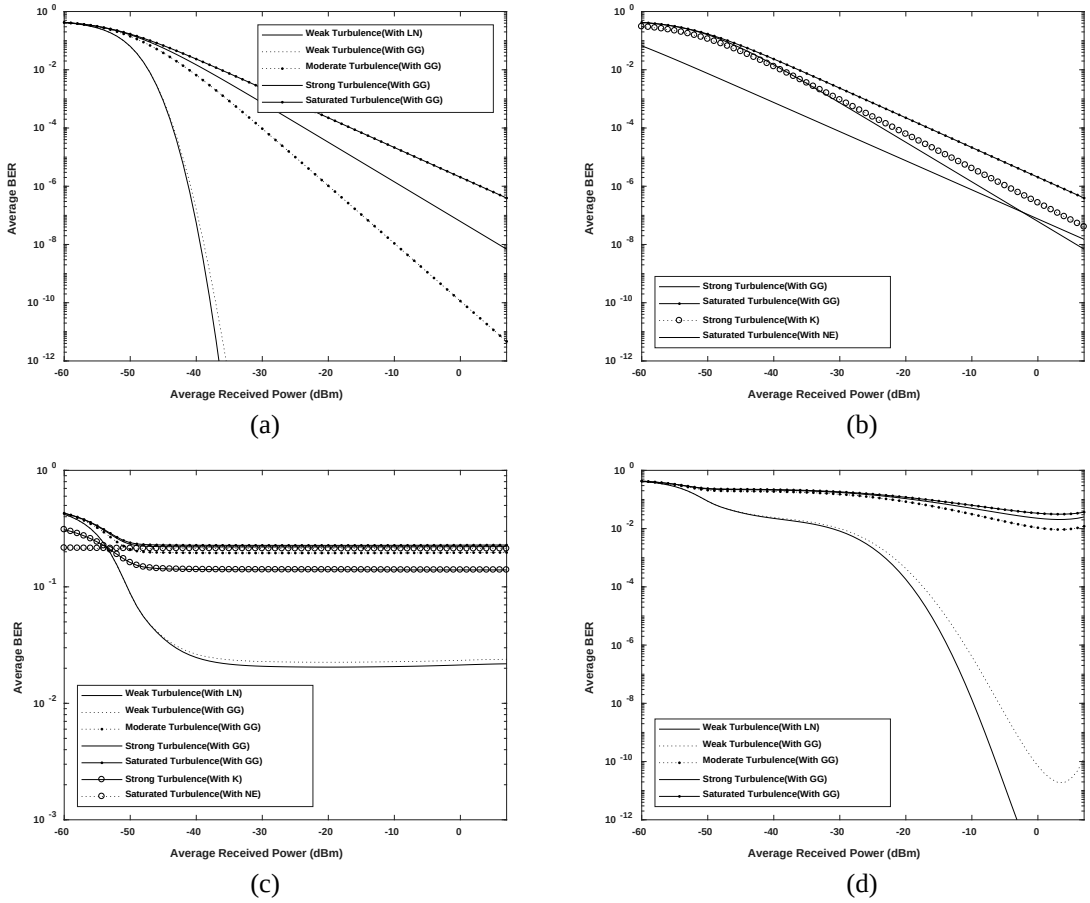

Figure 2: Average BER against average received power for different turbulence regimes (G_{ss} = 25 dB)
(a) Fixed gain preamplified receiver with an adaptive decision threshold
(b) Fixed gain preamplified receiver with an adaptive decision threshold
(c) Fixed gain preamplified receiver with non-adaptive decision threshold
(d) Saturated gain preamplified receiver with a non-adaptive decision threshold

In Figure 2(b) where a fixed gain preamplified receiver with an adaptive decision threshold is used, the GG distribution is used to describe the strong and saturated turbulence regimes, the K turbulence distribution is used to describe the strong turbulence regime and the NE turbulence distribution is used to describe the saturated turbulence regime. In the strong turbulence regime, the GG distribution is shown to perform better than the K

distribution at higher received optical power values ($<$ -35dBm) and in the saturated turbulence regime, the NE distribution is shown to perform better than the GG distribution for all the received optical power values considered. It should however be noted that the overall BER performance ($<10^{-8}$) is not good enough for a reliable communication link. In order to have a more reliable communication link in the strong and saturated turbulence regimes, other performance optimising measures such as a forward error correction (FEC) technique with interleaving can be introduced [14, 18].

In Figure 2(c) where a fixed gain preamplified receiver with a non-adaptive decision threshold is used, the LN distribution is used to describe the weak turbulence regime and the GG distribution is used to describe the weak, moderate, strong and saturated turbulence regimes. Also, the K and the NE turbulence distributions were used to describe the strong and saturated turbulence regimes respectively. Unlike the BER values ($\approx 10^{-12}$) obtained in Figure 2(a) where an adaptive decision threshold is used, BER floors at high BER values ($>10^{-2}$) are obtained in all the turbulence regimes in Figure 2(c). The BER floors are obtained because of the inability of a non-adaptive decision threshold to adapt to fluctuations in the received optical signal. However, a non-adaptive decision threshold can be used to obtain better BER performances as shown in Figure 2(d).

In Figure 2(d) where a saturated gain preamplified receiver with a non-adaptive decision threshold is used, the LN distribution is used to describe the weak turbulence regime and the GG distribution is used to describe the weak, moderate, strong and saturated turbulence regimes. Unlike the poor BER performances shown in Figure 2(c) where a non-adaptive decision threshold was also used at the receiver, the introduction of a saturated gain preamplifier allows for improved BER performances shown in Figure 2(d). While all the BER results shown in Figure 2(c) were more than 10^{-2}, better BER results ($<10^{-10}$ for LN and GG) are shown in Figure 2(d). It is also noticed that the merits of using a saturated gain preamplified receiver is mainly evident in the weak turbulence regime as shown by the LN and GG distributions. A noticeable similarity between the results for a non-adaptive and an adaptive decision threshold is the better BER performance observed with the LN distribution compared to the GG distribution in the weak turbulence regime. As mentioned in earlier results and shown in Figure 2(d), when a saturated gain preamplified receiver with a non-adaptive decision threshold is used, optimal BER performances are obtained when the P_{sat} value of the preamplifier is comparable to the received optical power.

Figure 3 shows the BER curves for different G_{ss} values using a saturated gain preamplified receiver with a non-adaptive decision threshold. As shown in [16], Figure 3 clearly also shows that the BER performances reaches an optimal level when the power at the preamplifier input is comparable with the P_{sat} values. This attribute can also be seen to be consistent for the different G_{ss} values as shown in Figure 3. Also, the BER performance improves as the G_{ss} value increases since an increase in the G_{ss} value allows wider range of powers to be received while providing more gain to the input signal.

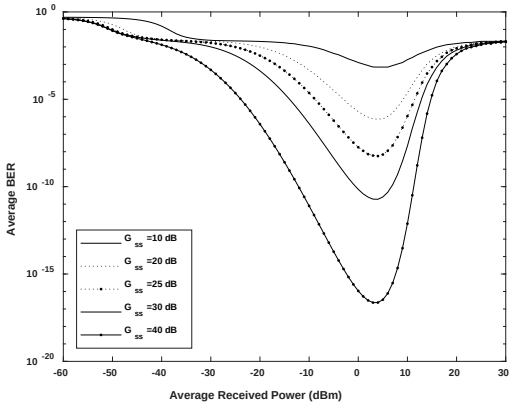

Figure 3: Average BER (using GG) against average received power for a saturated gain preamplified receiver with a non-adaptive decision threshold (σ_R^2 = 0.1, P_{sat} = 5 dBm)

While Figure 3 shows results for D_{rel} = 0.5, Figure 4 shows the minimum BER values that can be obtained at different threshold levels using a saturated gain preamplified receiver. As expected, the BER performance increases as the G_{ss} value increases. It is also observed that for all the various G_{ss} values, the best performances are obtained at $0.2 < D_{rel} < 0.3$.

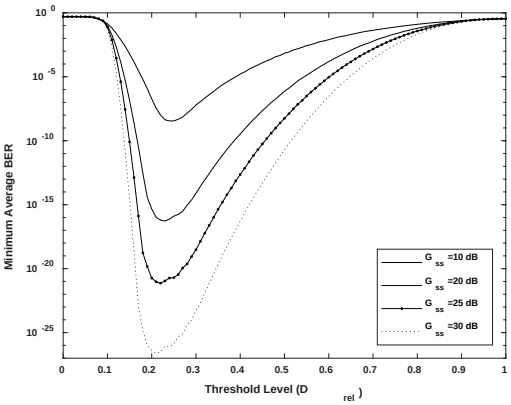

Figure 4: Minimum average BER (using GG) against threshold level for a saturated gain preamplified receiver using a non-adaptive decision threshold (σ_R^2 = 0.1, P_{sat} = 5 dBm).

6. CONCLUSION

This paper examined the performance of a fixed and saturated gain preamplified FSO communication system in a turbulent atmosphere. Results obtained in this paper showed that the LN distribution gives a better performance than the GG distribution in the weak turbulence regime. Also, as expected, the BER performance becomes better as the turbulence strength decreases. In the strong turbulence regime, the GG distribution is shown to perform better than

the K distribution at higher received optical power values and the NE distribution is shown to perform better than the GG distribution in the saturated turbulence regime. While the BER floors observed for a fixed gain preamplifier results shows that a non-adaptive decision threshold is unable to adapt to fluctuations in the received optical signal, the introduction of a saturated gain preamplifier allows for improved BER performances. In all the cases considered in this paper, the BER performances reaches an optimal level when the power at the preamplifier input is comparable with the internal saturation power of the preamplifier. It has also been shown that a gain saturated preamplified receiver performs optimally when the threshold level of the non-adaptive decision threshold is between 0.2 and 0.3.

REFERENCES

[1] Kedar, D. and Arnon, S. (2004). Urban optical wireless communication networks: the main challenges and possible solutions. *IEEE Communications Magazine*, 42(5), S2-S7.

[2] Carbonneau, T.H. and Wisely, D.R. (1998). Opportunities and challenges for optical wireless: the competitive advantage of free space telecommunications links in today's crowded marketplace, in *Wireless Technologies and Systems: Millimeter-Wave and Optical*, vol. 3232, 119-129.

[3] Szajowski, P., Nykolak, G., Auborn, J. J., Presby, H. M., and Tourgee, G. E. (1999). High power optical amplifier enable 1550 nm terrestrial free-space optical data-link operating@ 10 Gb/s, in *IEEE Military Communications Conference Proceedings*, vol. 1, 687-689.

[4] Hsu, V., Kahn, J.M. and Pister, K. (1998). Wireless communications for smart dust. Electronics Research Laboratory, College of Engineering, University of California.

[5] Popoola, W.O., Ghassemlooy, Z. and Ahmadi, V. (2008). Performance of sub-carrier modulated Free-Space Optical communication link in negative exponential atmospheric turbulence environment. *International Journal of Autonomous and Adaptive Communications Systems*, 1(3). 342-355.

[6] Popoola, W.O., Ghassemlooy, Z., Allen, J. I. H., Leitgeb, E., and Gao, S. (2008). Free-space optical communication employing subcarrier modulation and spatial diversity in atmospheric turbulence channel. *IET optoelectronics*, 2(1), 16-23.

[7] Chan, V.W. (2006). Free-space optical communications. *Journal of Lightwave Technology*, 24(12), 4750-4762.

[8] Andrews, L.C. and Phillips, R.L. (2005). *Laser Beam Propagation Through Random Media*. Vol. 52. Bellingham, WA: SPIE press.

[9] Xiaoming, Z. and Kahn, J.M. (2002). Free-space optical communication through atmospheric turbulence channels. *IEEE Transactions on Communications*, 50(8), 1293-1300.

[10] Arnon, S. (2003). Optimization of urban optical wireless communication systems. *IEEE Transactions on Wireless Communications*, 2(4), 626-629.

[11] Ghassemlooy, Z., Popoola, W.O. and Rajbhandari, S. (2012). *Optical Wireless Communications: System and Channel Modelling with MATLAB.* Boca Raton, FL 33487-2742: CRC Press.

[12] Bayaki, E., Michalopoulos, D.S. and Schober, R. (2012). EDFA-based all-optical relaying in free-space optical systems. *IEEE Transactions on Communications*, 60(12), 3797-3807.

[13] Andrews, L.C. and Phillips, R.L. (2004). Free-space optical communication link and atmospheric effects: single aperture and arrays, in *Free-Space Laser Communication Technologies XVI*, vol. 5338, 265-276.

[14] Xiaoming, Z. and Kahn, J.M. (2003). Performance bounds for coded free-space optical communications through atmospheric turbulence channels. *IEEE Transactions on Communications*, 51(8), 1233-1239.

[15] Khalighi, M., Schwartz, N., Aitamer, N., and Bourennane, S. (2009). Fading reduction by aperture averaging and spatial diversity in optical wireless systems. *Journal of optical communications and networking*, 1(6), 580-593.

[16] Bandele, O.J., Desai, P., Woolfson, M. S., and Phillips, A. J. (2016). Saturation in cascaded optical amplifier free-space optical communication systems. *IET Optoelectronics*, 10(3), 71-79.

[17] Ghassemlooy, Z., Popoola, W.O. and Leitgeb, E. (2007). Free-space optical communication using subearrier modulation in gamma-gamma atmospheric turbulence, in *9th International Conference on Transparent Optical Networks, 2007*, vol. 3, pp. 156-160.

[18] Aladeloba, A., Phillips, A. and Woolfson, M. (2012). Improved bit error rate evaluation for optically pre-amplified free-space optical communication systems in turbulent atmosphere. *IET optoelectronics*, 6(1), 26-33.

[19] Razavi, M. and Shapiro, J.H. (2003). Wireless optical communications via diversity reception and optical preamplification, in *IEEE International Conference on Communications, 2003, 4(3), 975-983.*

[20] Ramaswami, R., Sivarajan, K. and Sasaki, G. (2009). *Optical Networks: A Practical Perspective, 3rd Edition.* Morgan Kaufmann Publishers Inc. 925.

[21] Ribeiro, L.F.B., Da Rocha, J. and Pinto, J.L. (1995). Performance evaluation of EDFA preamplified receivers taking into account intersymbol interference. *Journal of Lightwave Technology*, 13(2), 225-232.

[22] Majumdar, A.K. (2005). Free-space laser communication performance in the atmospheric channel. *Journal of Optical and Fiber Communications Reports*, 2(4), 345-396.

[23] Akella, J., Yuksel, M. and Kalyanaraman, S. (2007). Multi-channel communication in free-space optical networks for the last-mile, in *15th IEEE Workshop on Local & Metropolitan Area Networks, 2007*, 43-48.